BiSON Birmingham Solar-Oscillations Network

TECHNICAL REPORT NO. 382

Fibre-feed tests at Mount Wilson in 2016 September

Steven J. Hale

The University of Birmingham, Edgbaston, Birmingham B15 2TT

2016 December 24

This technical report series is published by:

THE UNIVERSITY OF BIRMINGHAM

High-Resolution Optical-Spectroscopy Group

School of Physics and Astronomy
The University of Birmingham
Edgbaston, Birmingham B15 2TT, United Kingdom
Telephone: +44-121-414-4551

Fibre-feed tests at Mount Wilson in 2016 September

Steven J. Hale
The University of Birmingham, Edgbaston, Birmingham B15 2TT

2016 December 24

Abstract

A *Skywatcher HEQ5-Pro* motorised mount and *Starlight Express Superstar* CCD guide camera with OpenCV image processing were tested in use as a solar tracker. The best performance in RA and declination respectively was 0.00 ± 6.15 arcseconds and -1.32 ± 6.62 arcseconds. This compares favourably with data captured on the standard BiSON mount in Carnarvon where the RA precision was measured to be 0.158 ± 8.434 arcseconds and declination -0.066 ± 3.823 arcseconds. The spectrometer was temporarily modified to accept a fibre-feed from the new mount. A low-frequency "footprint" was present in the data residuals that was not resolved, but otherwise results were as expected and comparable to the standard network performance. Two WiFi access points were installed, providing coverage over the whole tower.

1 Introduction

Steven Hale visited Mount Wilson from 2016 September 13 to October 4. The last visit to Mount Wilson was in 2016 April to restart the systems for the summer, and to work on the guiding electronics and second-flat drive mechanism [1]. The purpose of this visit was to install and test a prototype optical-fibre based light collection system, and to temporarily modify the existing spectrometer to accept a fibre input.

It is not intended that this technical report provide significant detail on the hardware modifications or the software controlling the new telescope mount — this will be published in a later report. While the changes are briefly summarised here, the intention is only to present the results of the performance tests.

2 Mount and Guide Camera

After arriving on-site on September 13, the first four days of the visit were occupied entirely with installation of the new hardware. The mount is a *Skywatcher HEQ5-Pro* with a standard tripod. The fibre-collector and guider head attaches to the mount as a binocular arrangement. Both use 80 mm focal length objective lenses to form an image of the Sun approximately 0.7 mm in

(a) Skywatcher HEQ5-Pro mount.

(b) Fibre-collector and CCD camera.

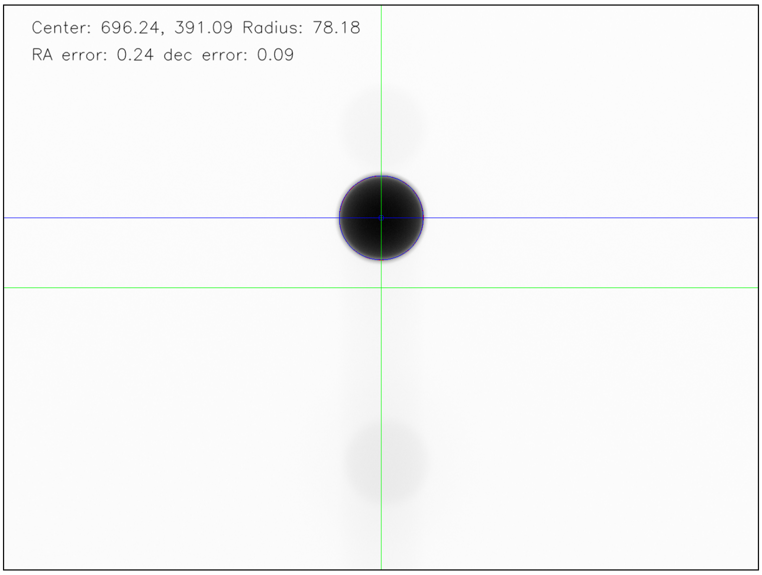

(c) Guider image processing with OpenCV.

Figure 1: Fibre-feed mount and telescope. The guider image has been inverted for printing.

diameter, with one focussing onto a 1.0 mm diameter optical-fibre and the other onto a *Starlight Express Superstar* CCD camera. The mount and telescope system are shown in Figure 1.

During the installation of the long optical-fibre down the entire length of the tower, there was concern that the fibre would not be able to support 60 feet of its own weight without breaking. To avoid this problem, the cable was unrolled into the shaft with both ends held at the top, meaning that at most 30 feet of cable was ever unsupported. This allowed the fibre to be cable-tied and supported at two points within the shaft, before one end of the cable was lowered all the way to the bottom using a length of string. The cable was installed successfully with no damage.

The mount was guided throughout the day by capturing images from the CCD camera and processing the position of the Sun using the OpenCV (Open-source Computer-Vision) library. An example of the image captured by the camera is shown in Figure 1c. Images were read from the camera as fast as possible — approximately once per second. The image exposure time is 79 ms. The image cadence limit is due to the CCD read-out time and USB transfer rate. The centroid position of the solar disc was found using OpenCV by applying a black and white threshold, finding the contours in the image, and subsequently reading out the contour centroid position. A measure of guiding error was determined by comparing the current solar position with the pixel values found when the solar image was observed to be directly on the centre of the fibre. The position error for each axis was then passed through a PID controller in order to determine the correct mount drive rate, and the mount updated with the new rate. The optics when mounted are short enough to allow the mount to move from the east horizon to the west horizon without requiring a meridian-flip at solar-noon, and so this greatly simplifies the mount control algorithm.

Currently the mount does not have any absolute position sensors installed and so it was required to manually point the system each morning. First light was achieved on September 17.

3 Modifications to Klaus for Fibre-Feed

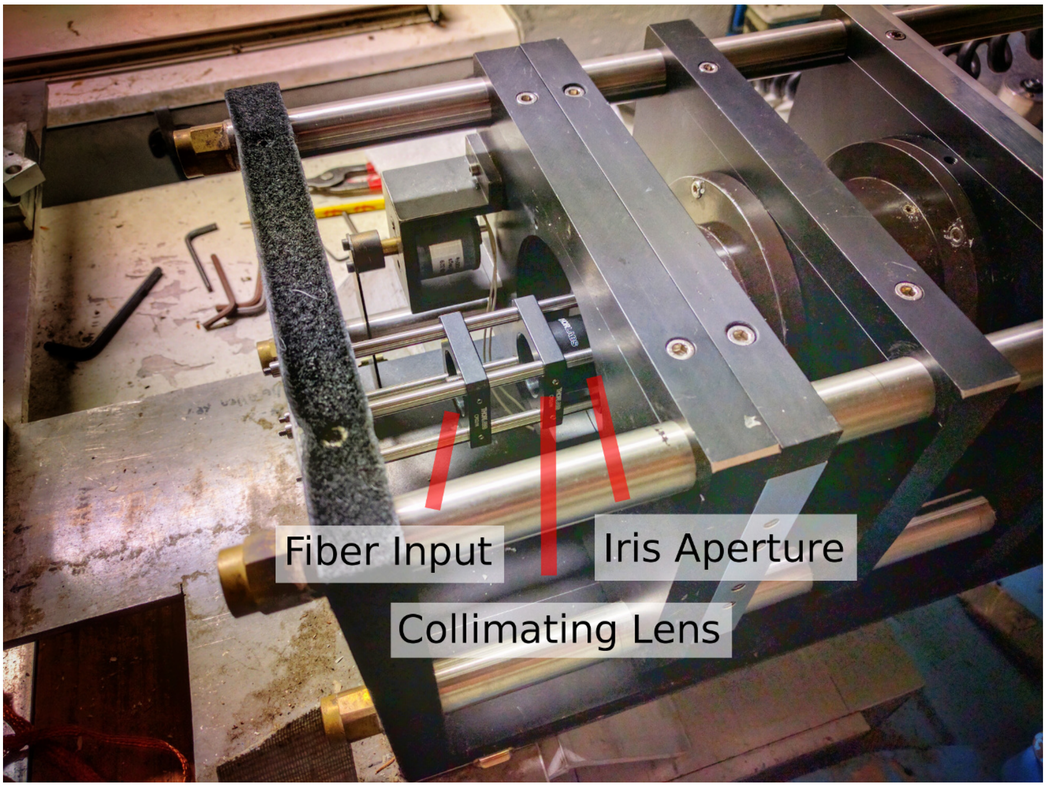

Figure 2: Fibre-feed modification to Klaus.

All the BiSON spectrometers are designed to point directly at the Sun. This is done by either swinging the spectrometer on an equatorial mount, or via mirrors using a coelostat. The conversion required to change "Klaus" from the standard direct-feed system to a fibre-feed system is quite simple. The front lens tube holds the pre-filters and two lenses in a telescope arrangement. The objective lens (L1) forms an image of the Sun, and a second lens (L2) re-collimates the light ready to be processed by subsequent optics. The entire front lens tube was removed and a new lens installed in the L2 position to collimate the output from a fibre, rather than collimate the image formed by an objective lens, after which the spectrometer operates as normal. An iris aperture was also installed to allow the beam intensity to be controlled and prevent the detectors from saturating. The optical modification as installed in "Klaus" are shown in Figure 2.

When installing the fibre and collimating lens, the focus of the system was checked using a 770 nm fibre-coupled LED as a light source. This was done by adjusting the position of the fibre relative to the focal point of the collimating lens and observing the beam size at L4, the lens immediately before the entrance to the first magnet and oven. The second magnet and oven has been removed from the chassis, and so it was also possible to check the beam focus at the position of the second vapour cell. It is very important to optimise the beam focus since this minimises the beam diameter, and so minimises the non-resonantly scattered light from the vapour cell. If the beam is too large, then it has the effect of lighting up the entrance through the magnet and significantly increasing the cold-counts, reducing the instrument sensitivity.

The intensity of the LED was controlled to ensure the scattering-detectors were just below saturation with the vapour-cell hot, and then the hot-to-cold ratio was measured. The starboard detector measured 57.7k counts cold, and 450.9k counts hot, a ratio of 7.8. The port detector measured 62.0k counts cold, and 491.2k counts hot, a ratio of 7.9.

When tested with real sunlight both scattering-detectors saturated very quickly. This is due to the fibre-collector using a slightly larger objective aperture than the original Klaus telescope system, and also the new coarse red-filter having better transmission at 770 nm. A 30 mm cardboard aperture matching the original diameter was fabricated and installed on the fibre-collector, and the internal iris-aperture also reduced to bring the intensity within the dynamic range of the detectors. The hot-to-cold ratio was measured again and with real sunlight this had reduced to 3.6 for starboard and 3.9 for port. It is expected that this could be significantly improved by reducing the detector gains and removing the apertures, similar to the tests using the fibre-coupled LED.

Klaus was returned to the standard mirror-fed configuration on September 30. The hot-to-cold ratio remained at 3.7 for starboard and 4.0 for port, similar to that achieved with the fibre on September 18.

4 Performance Tests

(a) Radio antenna

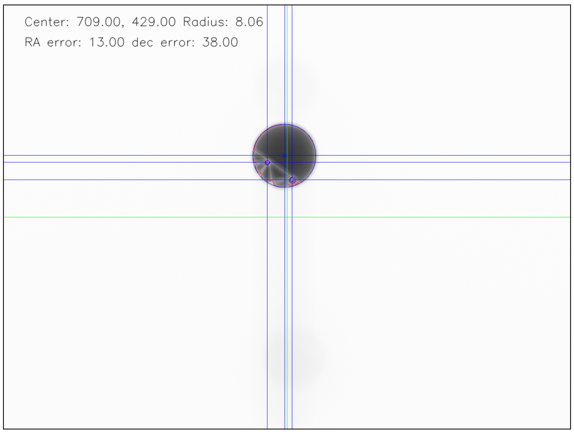

(b) Guider shadow

Figure 3: Radio antenna shadowing.

The first test of the new system was on September 17. Most of the day was taken finalising the PID guiding functions, and so only three hours of data were collected in the afternoon. The data, shown in Figure 4, suffer a oscillation at 8.165 mHz but otherwise look very good. Shortly before sunset, the Sun passed behind one of the radio towers to the west of the observatory, shown in Figure 3, causing a temporary issue with guiding.

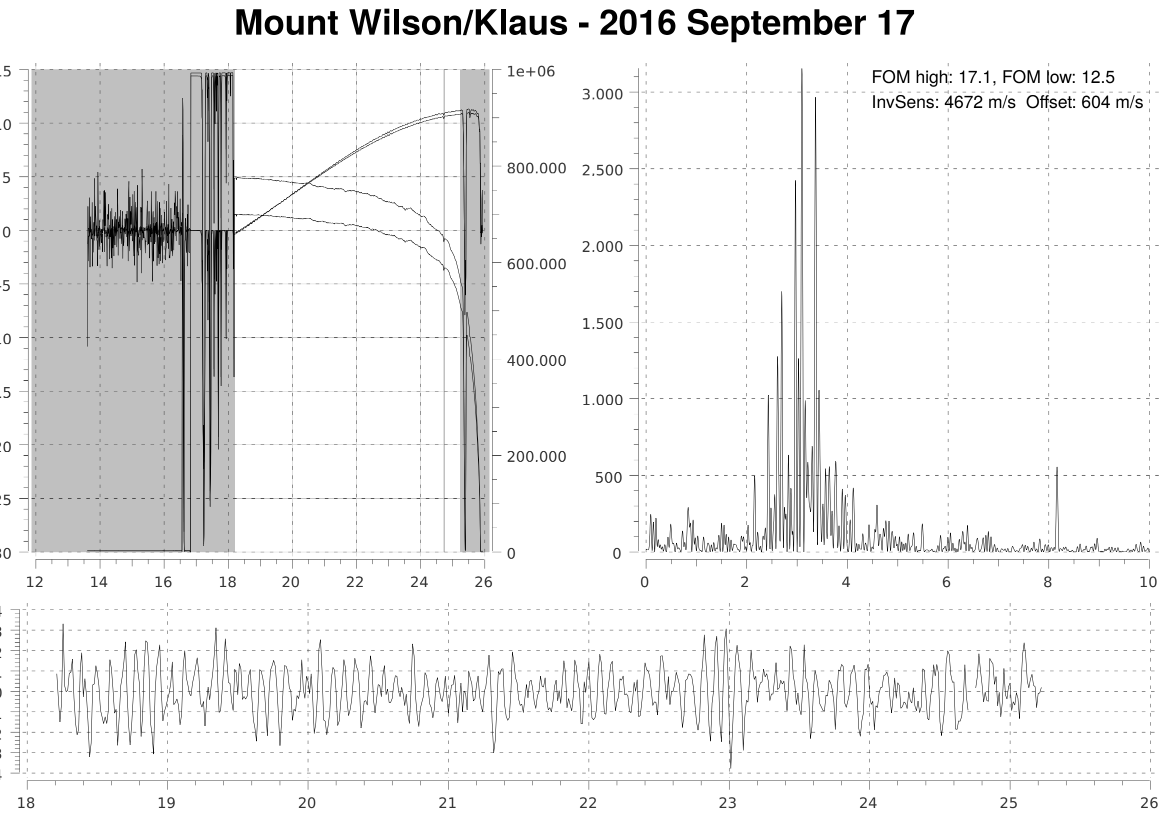

Figure 4: 2016 September 17

Weather was poor over the next few days, with only two hours of data collected on both September 18 and September 21, shown in Figures 5 and 6 respectively. A full day of data was acquired on September 23, show in Figure 7, although some high level haze resulted in poor quality.

A further four days of data were acquired before it was time to restore Klaus to the original mirror-fed configuration. Additional guider telemetry logging was also added in order to assess the guider performance and stability. Results from September 24 are shown in Figures 11. The cause of the low-frequency drifts in the residuals is not clear. It is possibly a footprint-like problem which has been previously solved by tilting the front coarse red filter, and so the cause is most likely back-reflections somewhere in the system. The RA proportional gain was reduced which eliminated the 8.165 mHz guider oscillation. The jumps in RA position error shortly after sunrise and shortly before sunset, shown in Figure 8, are due to backlash in the RA drive-train as the telescope weight shifts on the axis. Both axes have a minimum drive rate of 6 microsteps-per-second, and this is visible in the declination drive rate, Figure 9, where the PID control becomes essentially an on/off switch at minimum-rate around zero-error. The distribution of position-error for both axes, calibrated in arcseconds, is shown in Figure 10.

Several different guider PID coefficients were tested over the next few days. Results from September 25 are shown in Figure 15, 12, 13, and 14.

Results from September 26 are shown in Figure 19, 16, 17, and 18. At the end of the day the movement of the declination axis was found to be very notchy. The movement cleared as the axis was manually exercised several times through the full range of motion. The is possibly the cause of the slightly asymmetric error distributions on the declination axis.

Results from September 29 are shown in Figure 23, 20, 21, and 22. The morning was clear, but became cloudy in the afternoon.

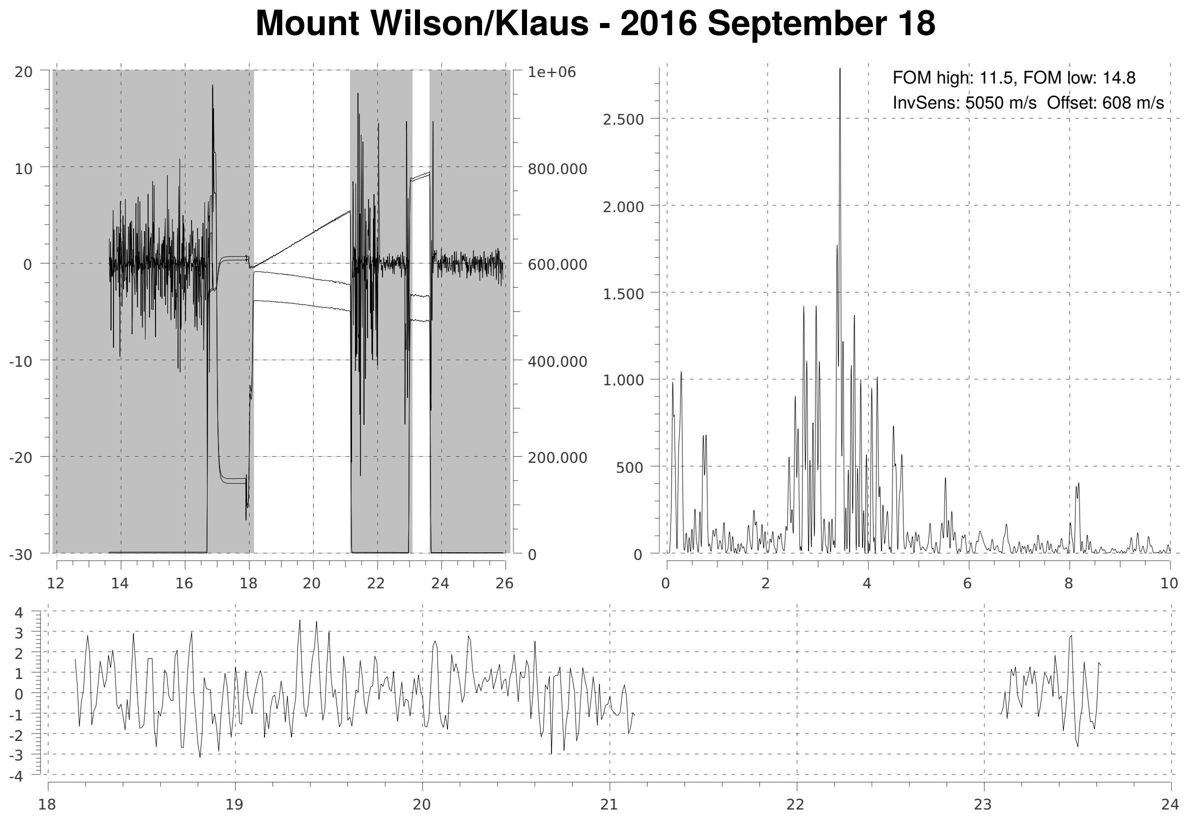

Figure 5: 2016 September 18

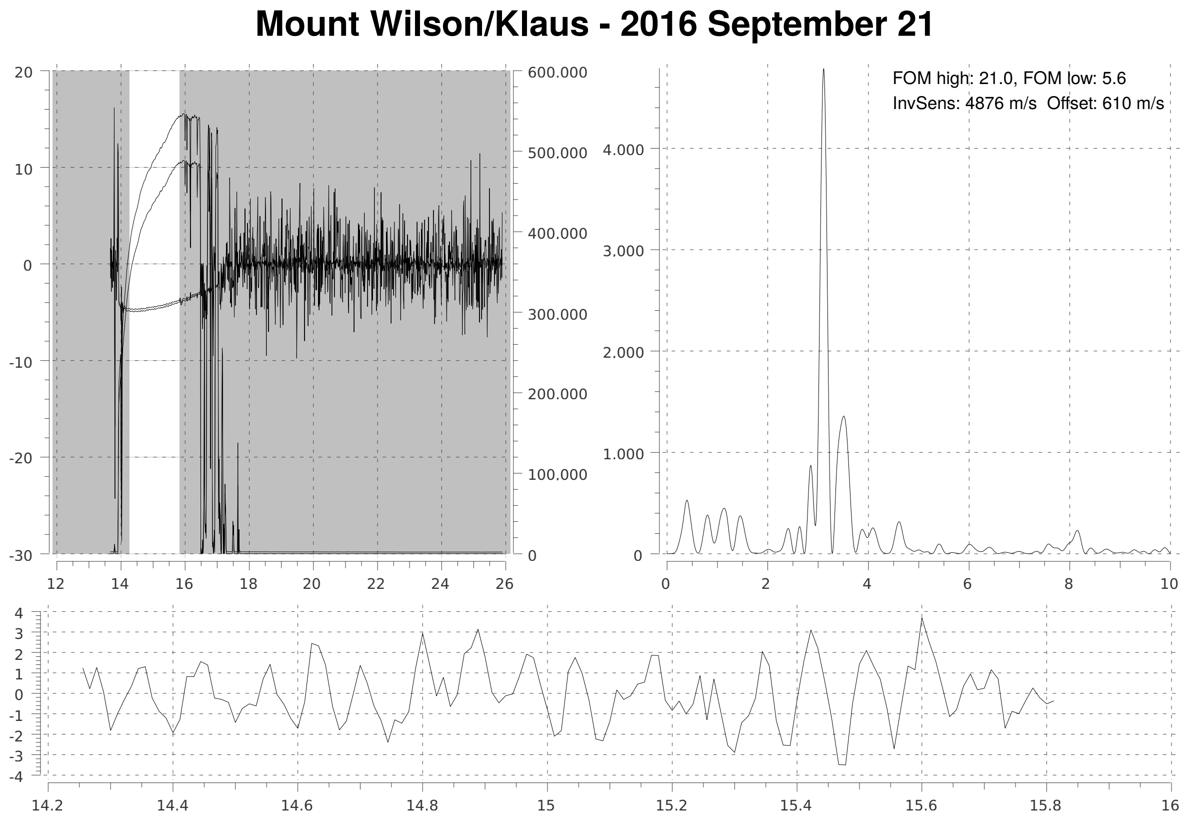

Figure 6: 2016 September 21

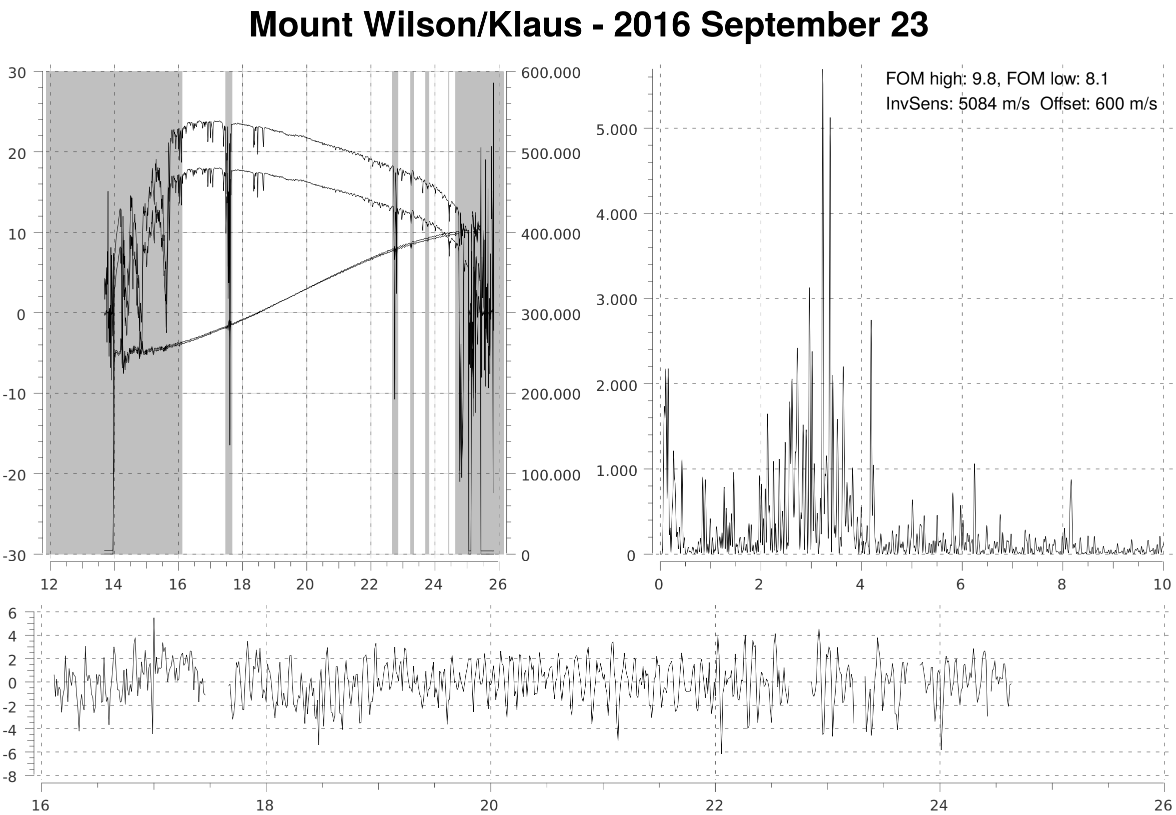

Figure 7: 2016 September 23

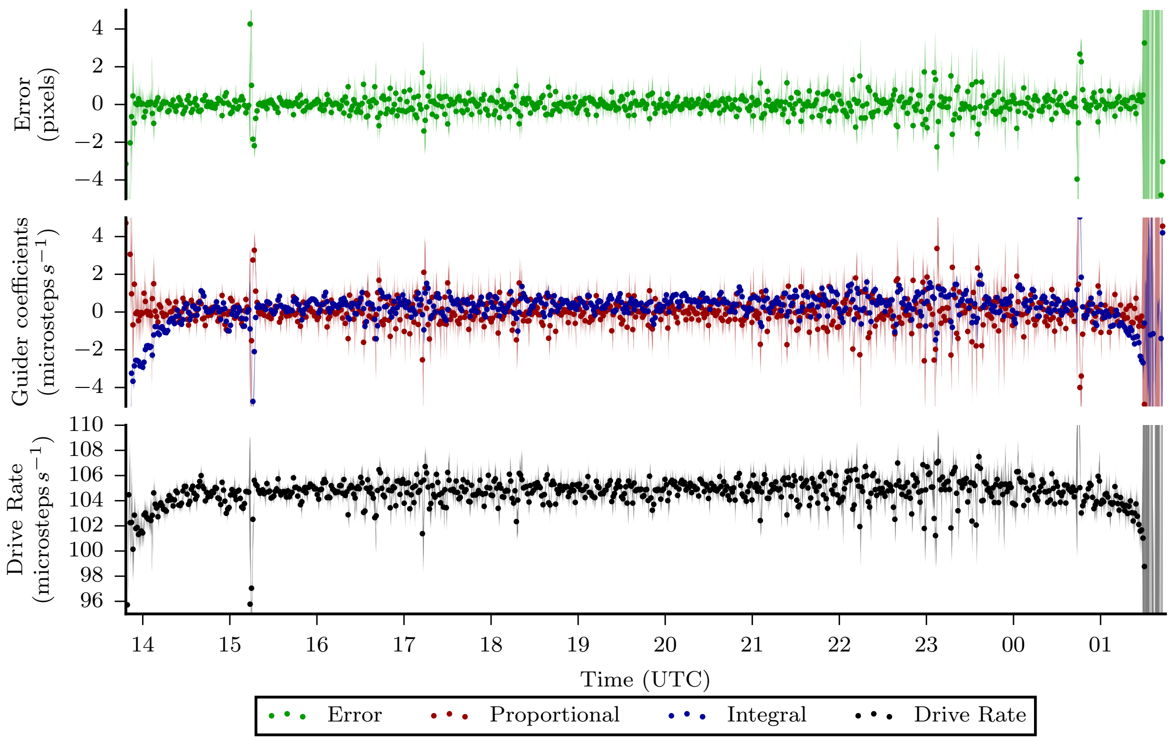

Figure 8: Guider RA performance on 2016 September 24. Each dot represents the median of 50 points, and the banding represents ±1 sigma on each median value.

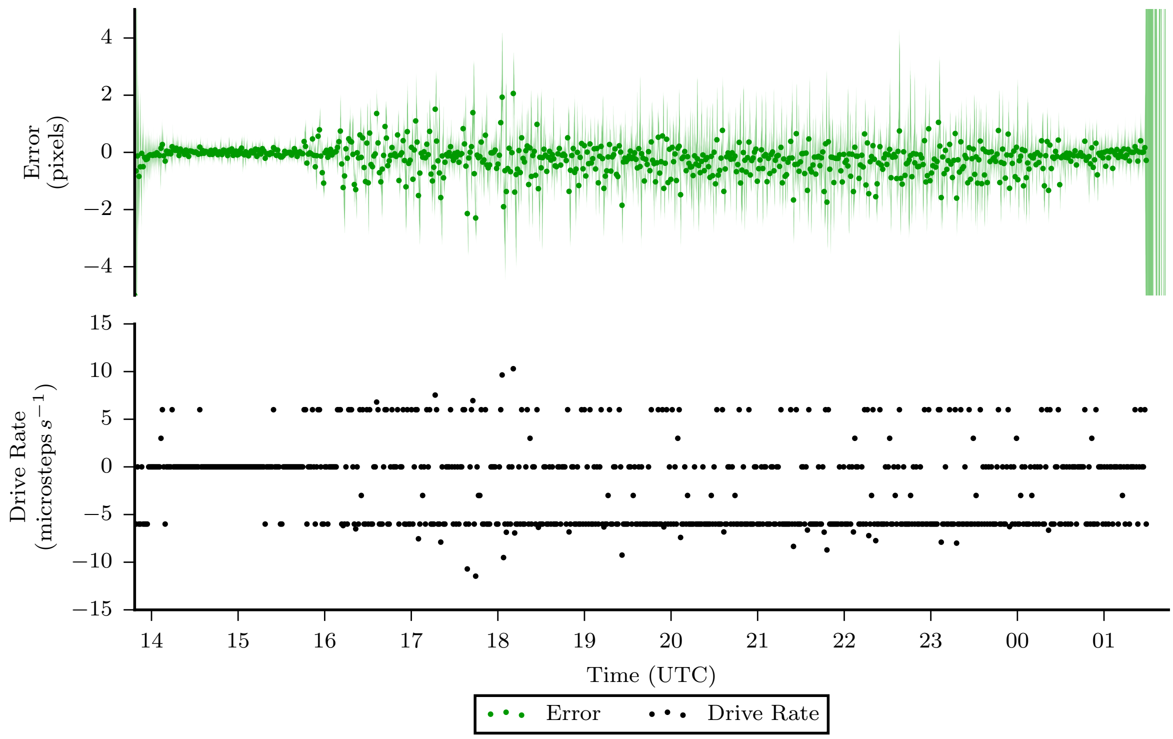

Figure 9: Guider declination performance on 2016 September 24. Each dot represents the median of 50 points, and the banding represents ±1 sigma on each median value.

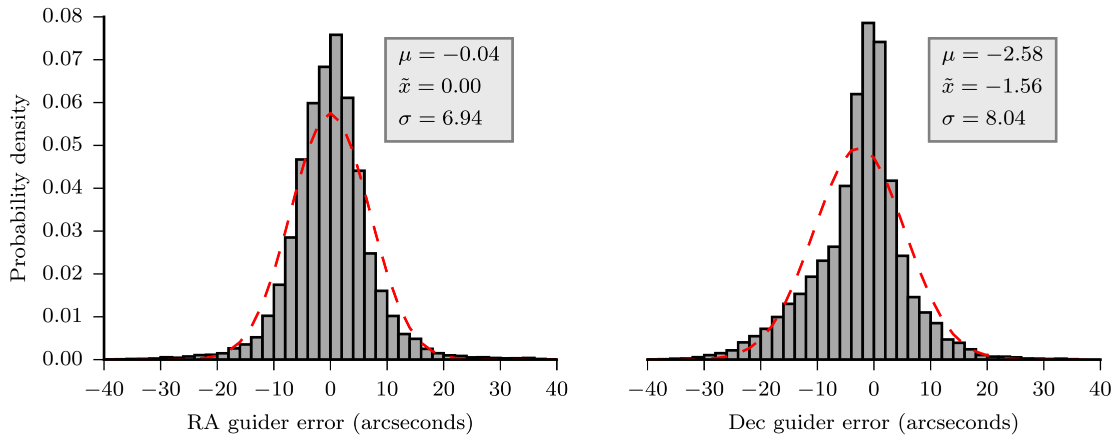

Figure 10: Guider performance histogram on 2016 September 24. The dashed red line indicates the equivalent Gaussian for the measured median and standard deviation.

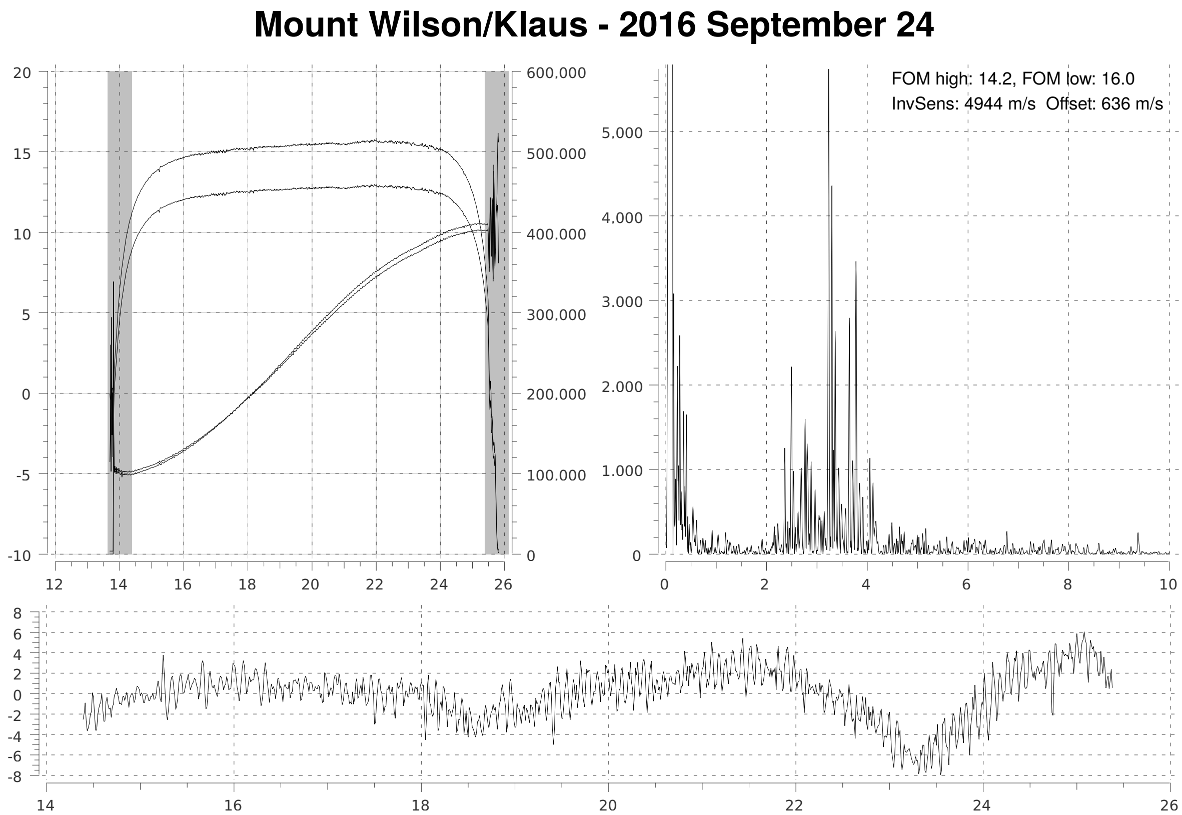

Figure 11: 2016 September 24

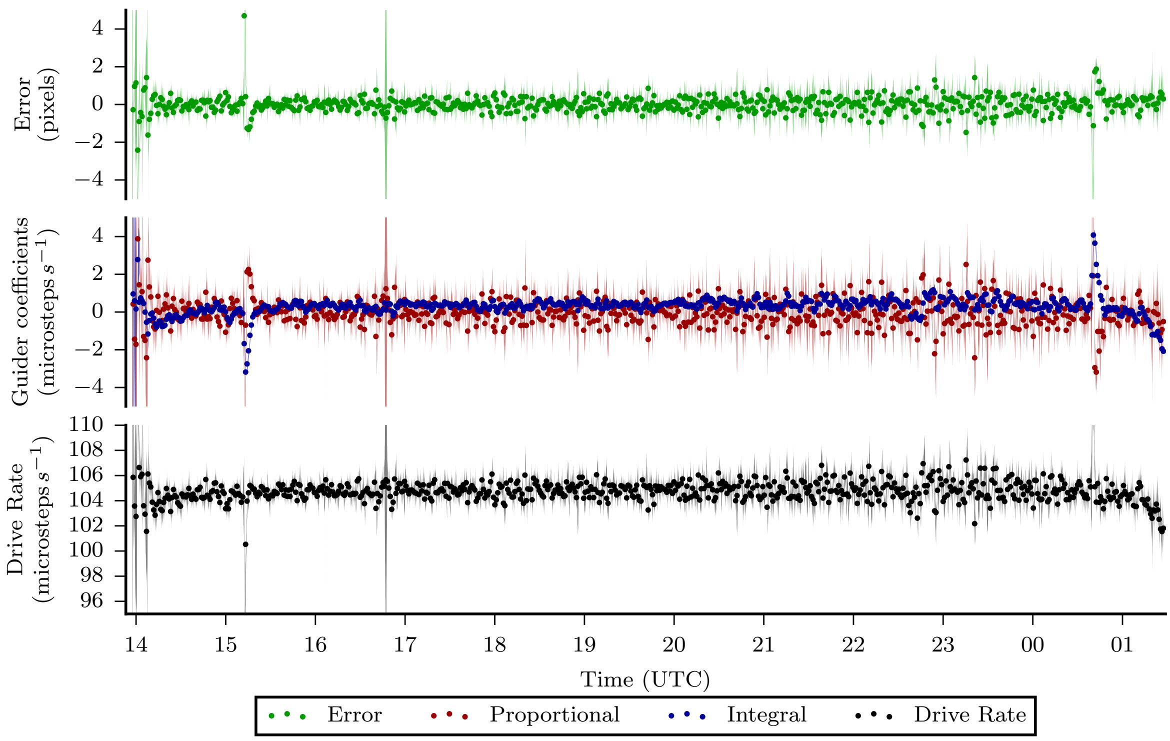

Figure 12: Guider RA performance on 2016 September 25. Each dot represents the median of 50 points, and the banding represents ±1 sigma on each median value.

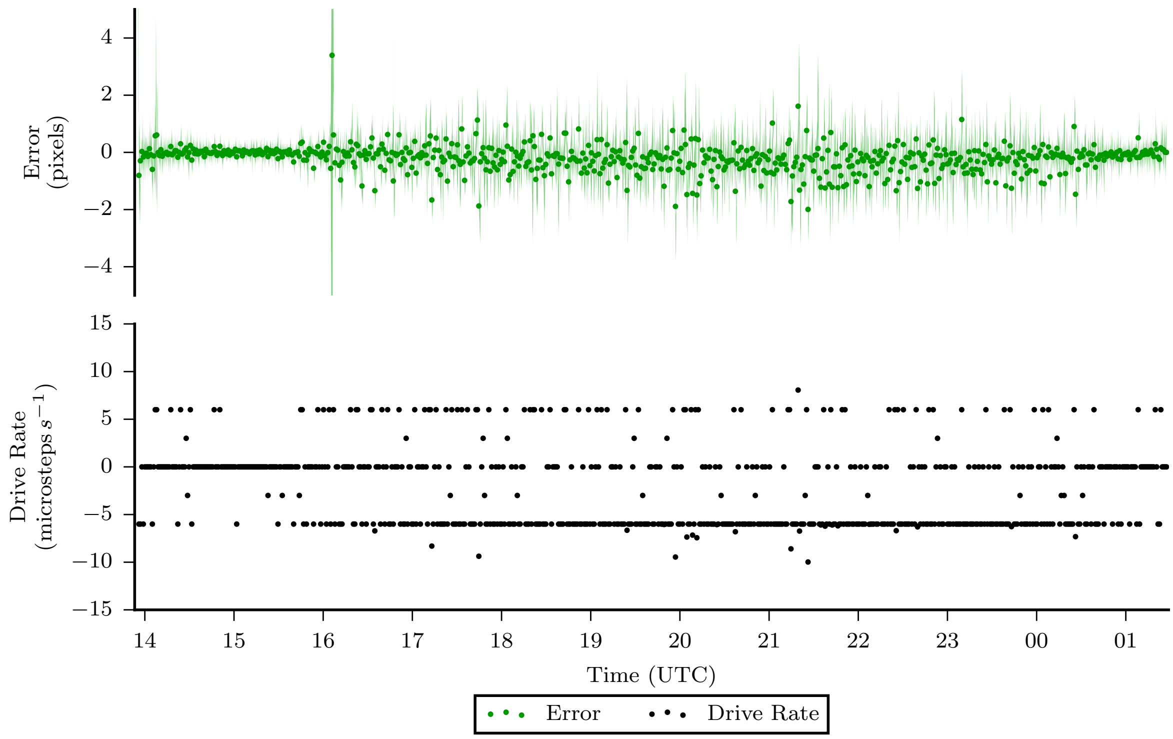

Figure 13: Guider declination performance on 2016 September 25. Each dot represents the median of 50 points, and the banding represents ±1 sigma on each median value.

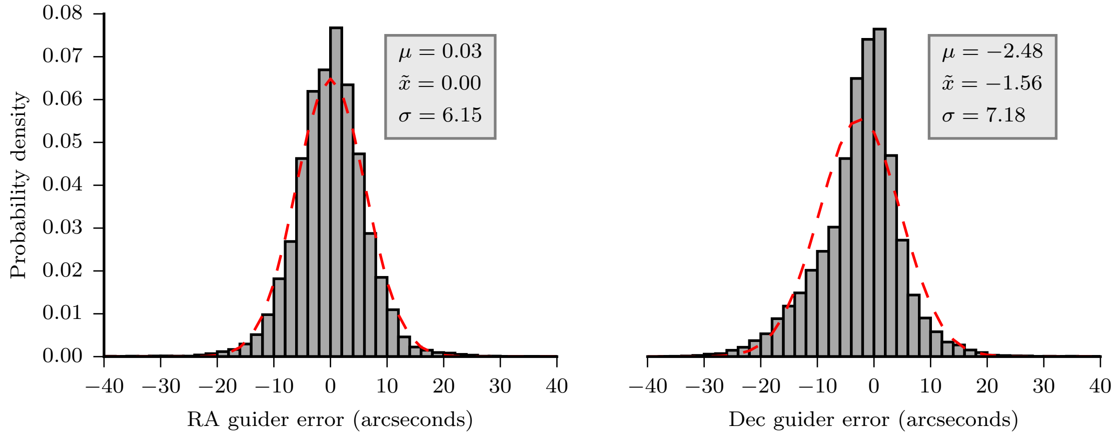

Figure 14: Guider performance histogram on 2016 September 25. The dashed red line indicates the equivalent Gaussian for the measured median and standard deviation.

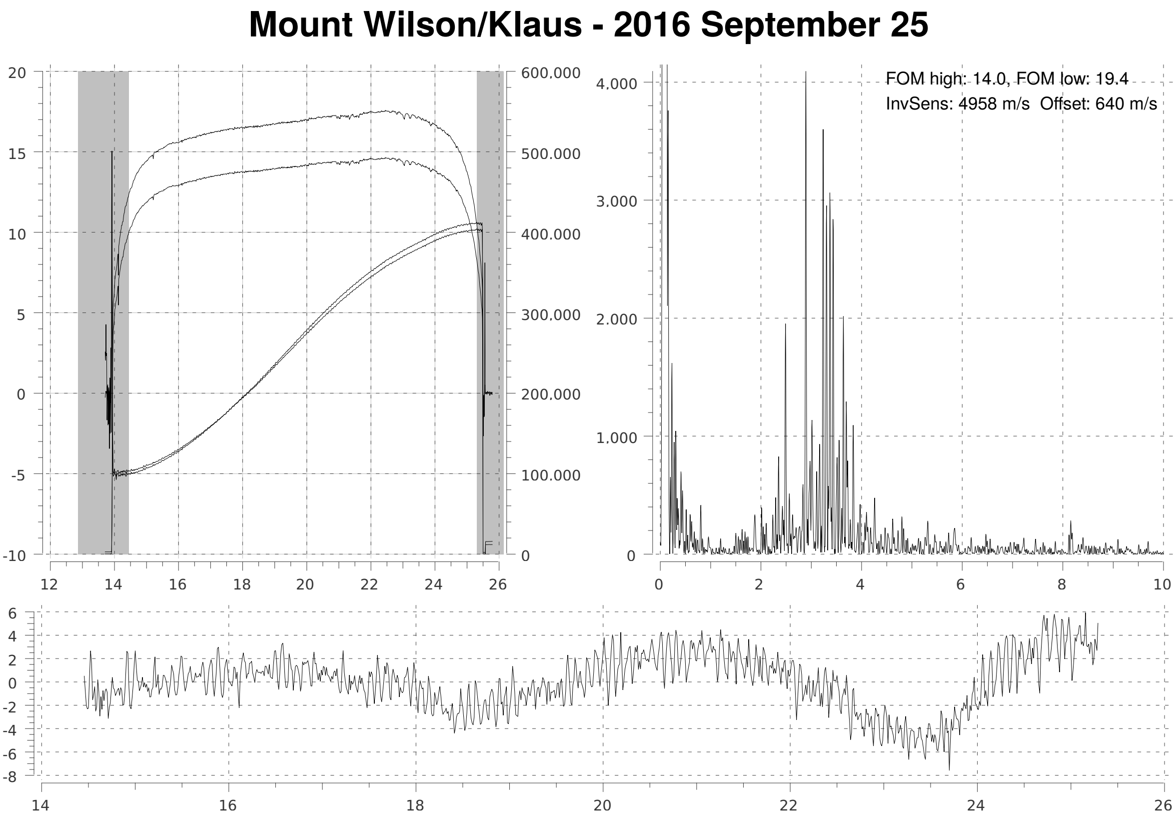

Figure 15: 2016 September 25

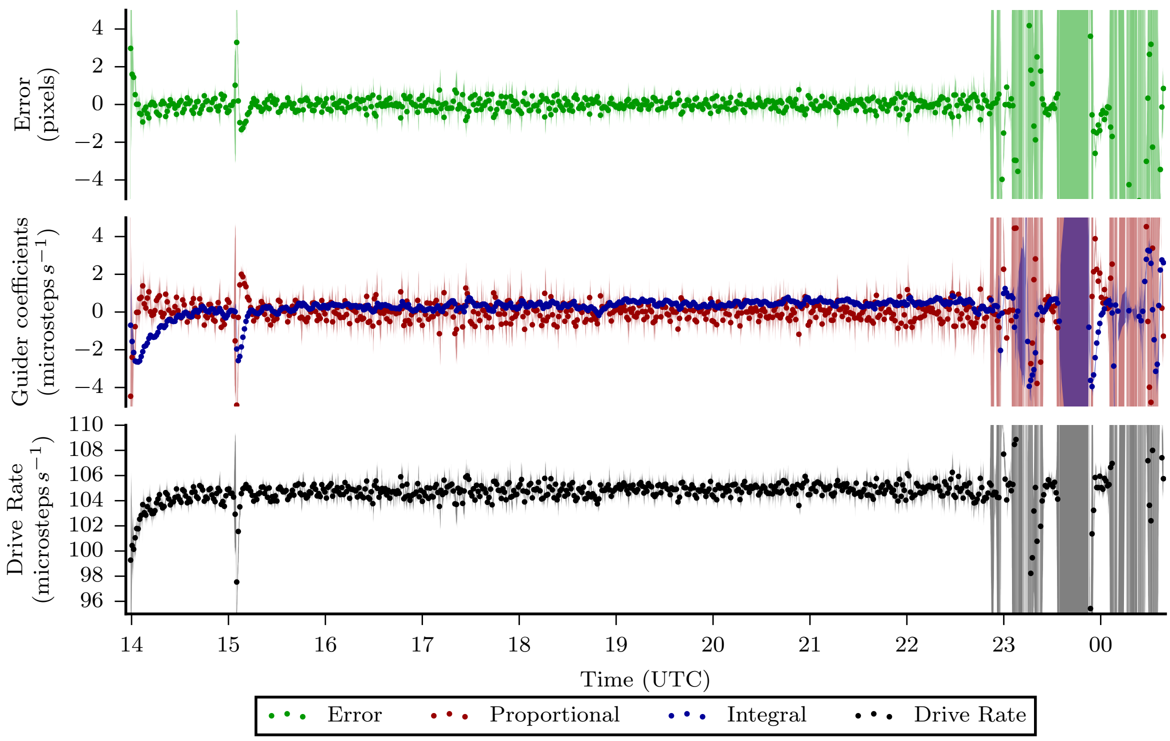

Figure 16: Guider RA performance on 2016 September 26. Each dot represents the median of 50 points, and the banding represents ±1 sigma on each median value.

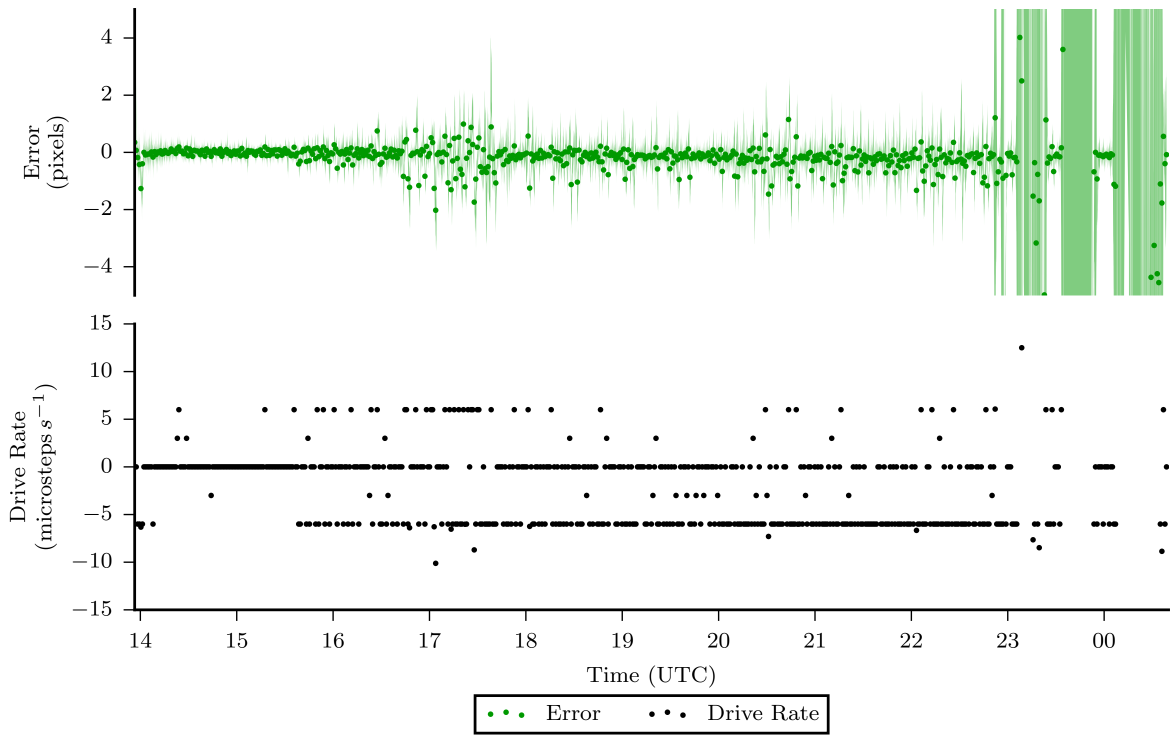

Figure 17: Guider declination performance on 2016 September 26. Each dot represents the median of 50 points, and the banding represents ±1 sigma on each median value.

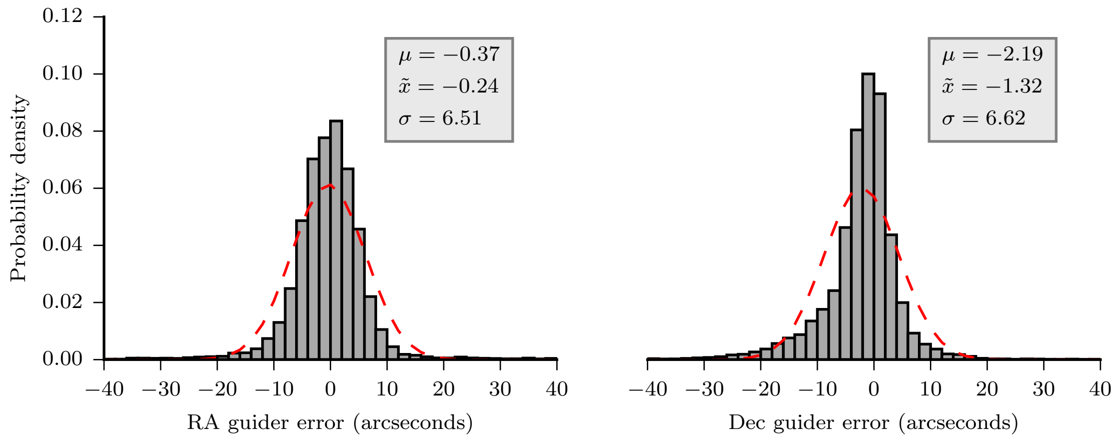

Figure 18: Guider performance histogram on 2016 September 26. The dashed red line indicates the equivalent Gaussian for the measured median and standard deviation.

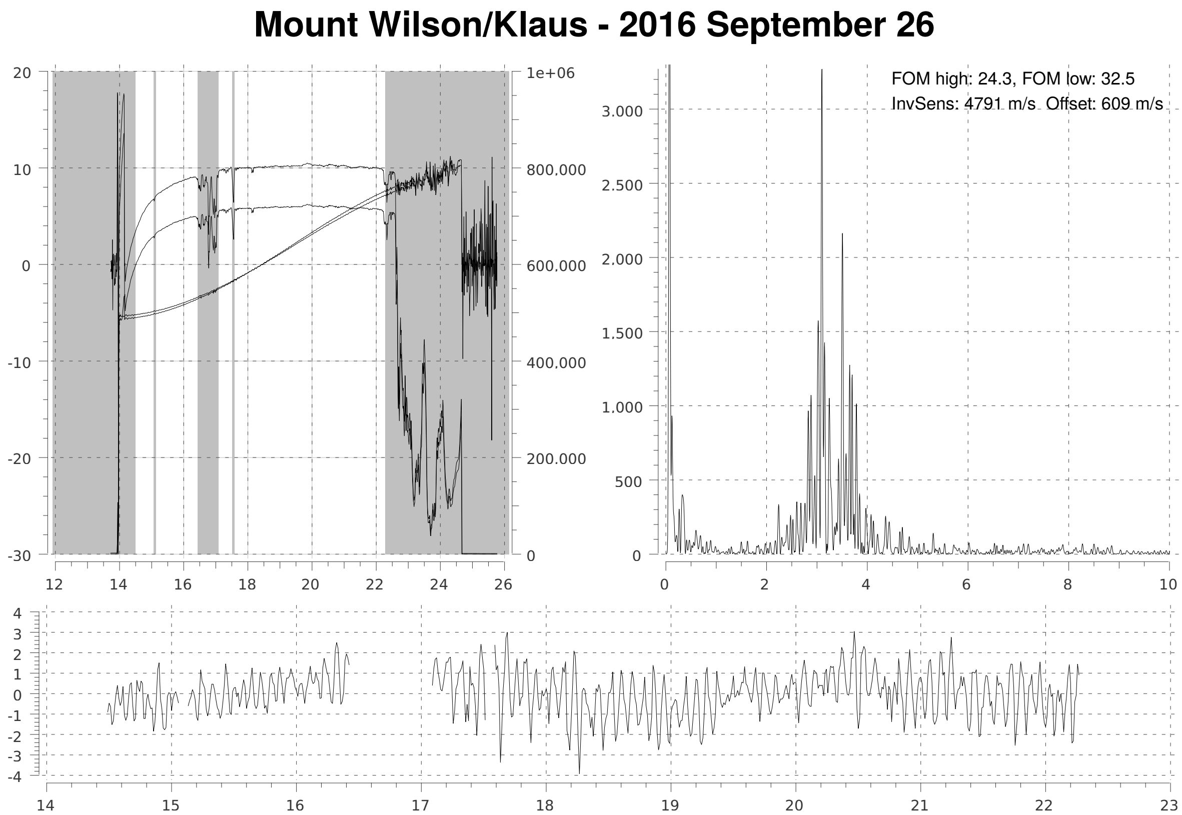

Figure 19: 2016 September 26

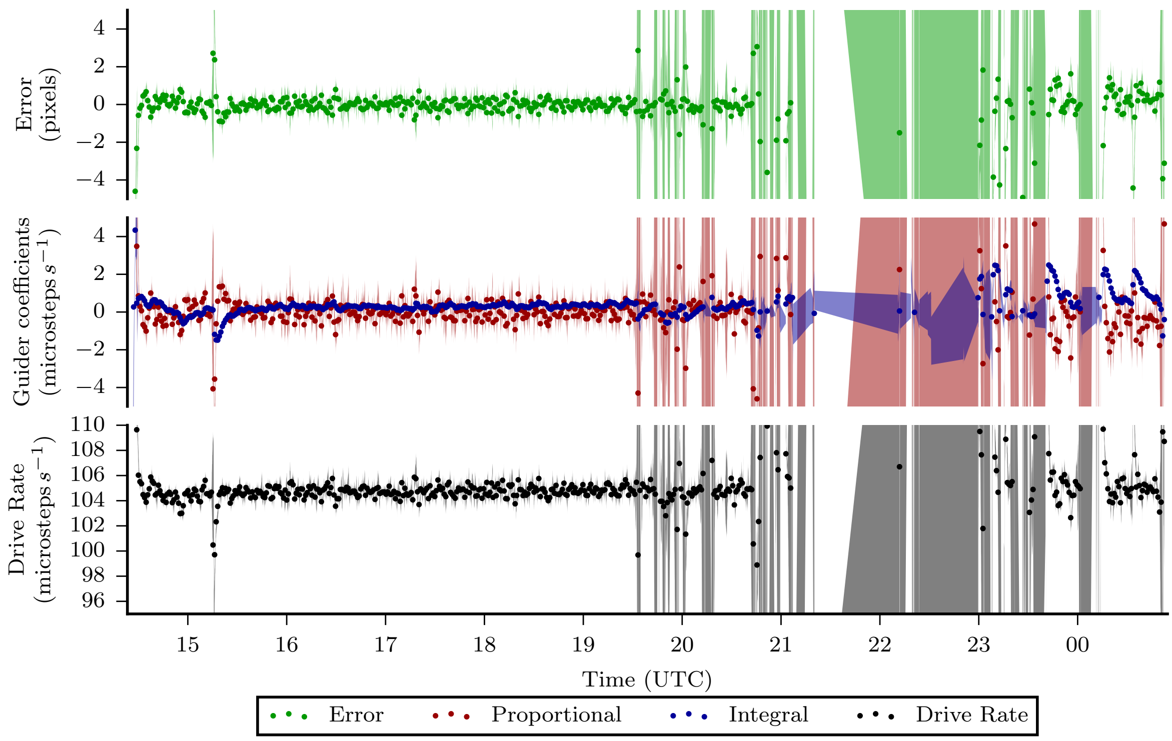

Figure 20: Guider RA performance on 2016 September 29. Each dot represents the median of 50 points, and the banding represents ±1 sigma on each median value.

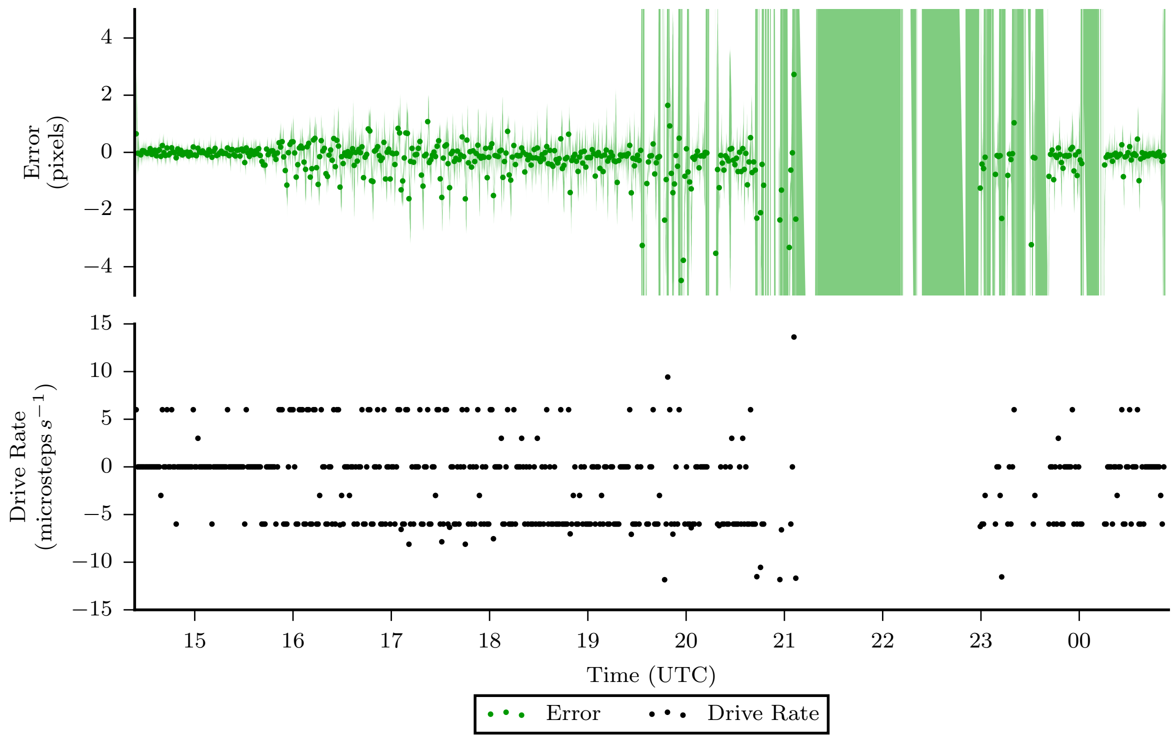

Figure 21: Guider declination performance on 2016 September 29. Each dot represents the median of 50 points, and the banding represents ±1 sigma on each median value.

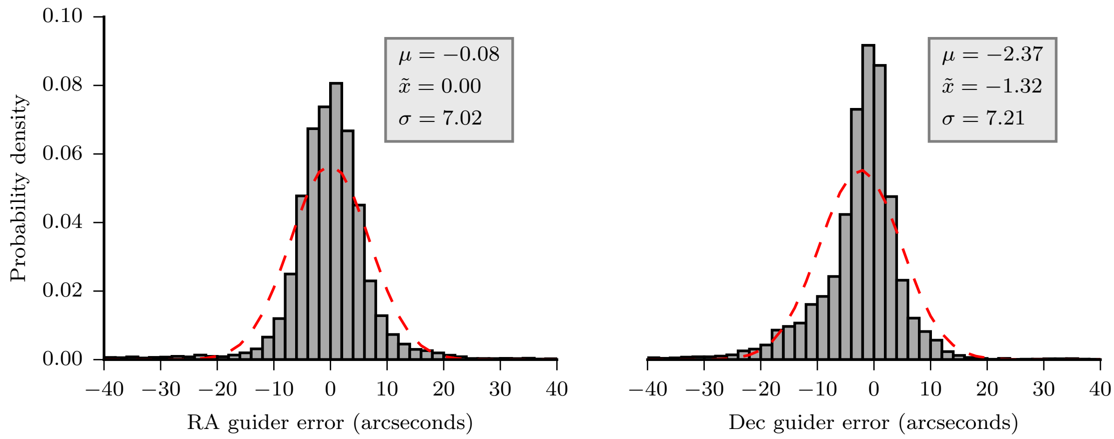

Figure 22: Guider performance histogram on 2016 September 29. The dashed red line indicates the equivalent Gaussian for the measured median and standard deviation.

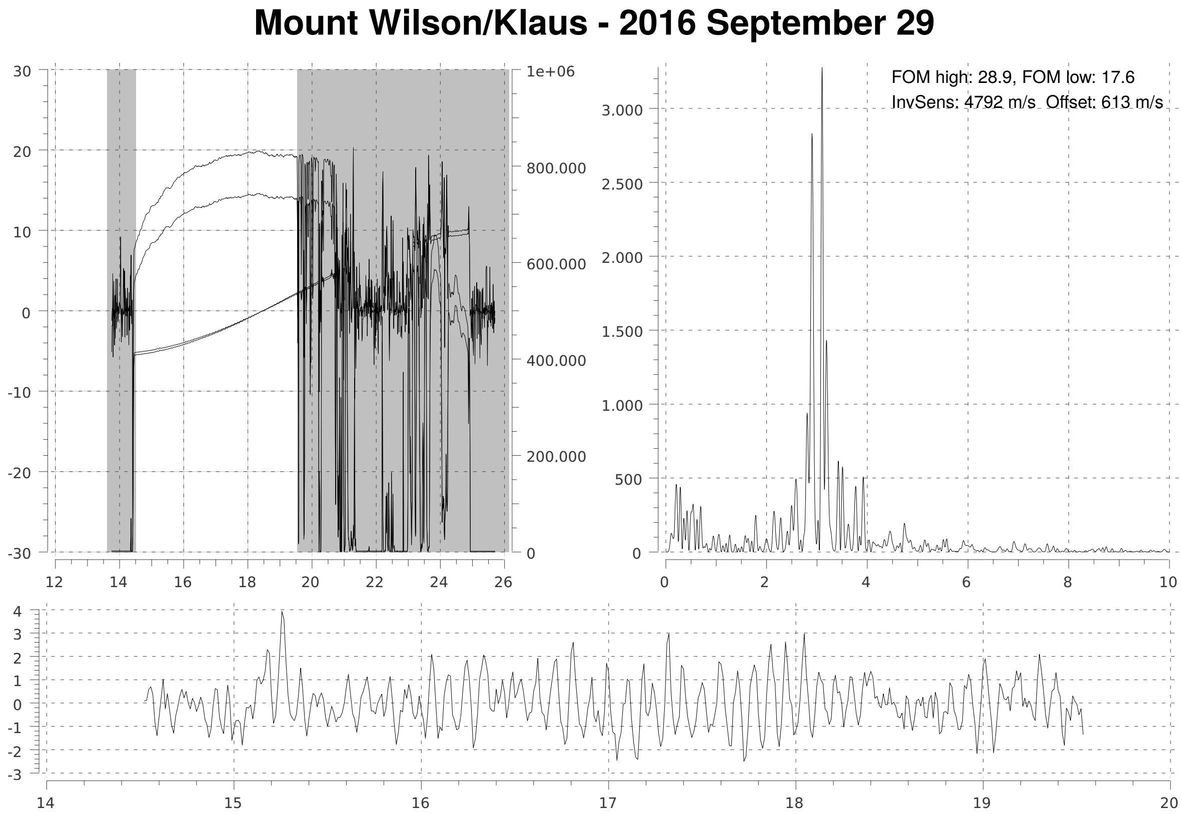

Figure 23: 2016 September 29

The guider performance statistics are summarised in Table 1 and 2. The best performance in RA was achieved on September 25 with a precision of 0.00 ± 6.15 arcseconds. The best performance in declination was achieved on September 26 with a precision of -1.32 ± 6.62 arcseconds. This compares favourably with data captured on the standard BiSON mount in Carnarvon on 2016 August 16 [2], where the RA precision was measured to be 0.158 ± 8.434 arcseconds and declination -0.066 ± 3.823 arcseconds.

Table 1: RA guider parameters and performance results.

Date	k_p	k_i	Mean	Median arcseconds	Sigma
September 17	-1.9	-0.007			
September 18	-1.9	-0.007			
September 21	-1.9	-0.007			
September 23	-1.9	-0.007			
September 24	-1.5	-0.02	-0.04	0.00	6.94
September 25	-1.7	-0.01	-0.03	0.00	6.15
September 26	-1.5	-0.007	-0.37	-0.24	6.51
September 29	-1.5	-0.005	-0.08	0.00	7.02

Table 2: Declination guider parameters and performance results.

Date	k_p	k_i	Mean	Median arcseconds	Sigma
September 17	1.9	0.0			
September 18	1.9	0.0			
September 21	1.9	0.0			
September 23	1.9	0.0			
September 24	5.0	0.0	-2.58	-1.56	8.04
September 25	5.0	0.0	-2.48	-1.56	7.18
September 26	5.0	0.0	-2.19	-1.32	6.62
September 29	5.0	0.0	-2.37	-1.32	7.21

5 WiFi Access Points

Two wireless access points were installed in the tower. There is one in the control room plugged into a ethernet switch. The second is at the top of the tower acting as a repeater for the first. The whole tower now has good WiFi coverage.

References

[1] Hale, S. J. Autoguider repairs at Mount Wilson in 2016 April. *BiSON Technical Report Series,* Number 380, High-Resolution Optical-Spectroscopy Group, University of Birmingham, UK, 2016. URL `http://epapers.bham.ac.uk/3132/`. [page 1]

[2] Hale, S. J. Repairs to Jabba at Carnarvon in 2016 August. *BiSON Technical Report Series,* Number 381, High-Resolution Optical-Spectroscopy Group, University of Birmingham, UK, 2016. URL `http://epapers.bham.ac.uk/3133/`. [page 15]